JEE Journal of Ecological Engineering

Journal of Ecological Engineering, 2026, 27(1), 325–341
https://doi.org/10.12911/22998993/210143
ISSN 2299–8993, License CC-BY 4.0

Received: 2025.08.20
Accepted: 2025.10.01
Published: 2025.11.25

Sustainable production of (Ca/Al)-layered double hydroxide -alginate beads for remediation of water contaminated with amoxicillin antibiotic

Anfal Enad Khalaf[1*], Ayad A.H. Faisal[1]

[1] Department of Environmental Engineering, College of Engineering, University of Baghdad, Baghdad, Iraq
* Corresponding author's e-mail: anfal.enad2311@coeng.uobaghdad.edu.iq

ABSTRACT

This work concentrates on the synthesis nano-sized calcium and aluminum layered double hydroxide (LDH) from environmental wastes and industrial by-products. Cement kiln dust (CKD) was used as a source of calcium, and waterworks treatment sludge (WTS) from water treatment plants was used as a source of aluminum. The (Ca/Al)-LDH nanoparticles have synthesized by co-precipitation method to produce a new sorbent. (Ca/Al)-LDH nanoparticles must be immobilized using sodium alginate to obtain the spherical forms named (Ca/Al)-LDH-alginate beads that were tested for the elimination of amoxicillin (AMX) antibiotic from the aquatic environment. The optimal conditions for the production of LDH that achieved the highest adsorption (calcium /aluminum ratio, pH, and the percentage of LDH in alginate beads) were studied to verify its adsorption efficiency. The study demonstrated that it is possible to remove approximately 52% of AMX under optimal synthesis conditions, which include a 1:1 ratio of Ca:Al, 20% LDH in alginate, and pH of 10. The LDH was characterized using SEM, XRD, FT-IR, EDX, TEM, and BET tests. The results demonstrate that the (Ca/Al)-LDH was formed with a unique geometric structure with surface area of 48.55 m^2/g. Batch tests demonstrated that more than 94% of AMX can be removed with 90 minutes, pH 3, sorbent amount 0.5 g/50 mL, and speed 250 rpm, for AMX initial concentration 50 mg/L, to achieve the highest sorption capacity of 17.47 mg/g. The pseudo-second order model was used to measure the kinetic tests, and as a result, the removal process will primarily rely on the chemisorption mechanism. The regeneration process proved the possibility of using exhausted beads for ten cycles with efficiency greater than 86%.

Keywords: amoxicillin adsorption, layered double hydroxide, cement kiln dust; alum waste.

INTRODUCTION

The driving key for sustainable development was highlighted in the UN Sustainable Development Goals and was well-identified as Goal 6 for the availability of clean and sanitary water (Johnston et al., 2021). Pollutants in water are classified into inorganic pollutants, which are mainly related to the presence of metallic elements (e.g., Zn^{+2}, Pb^{+2}), and organic pollutants such as antibiotics (Prasse et al., 2010). Amoxicillin (AMX) is one of the organic pollutants in water that exists due to its continuous use by humans as a broad-spectrum antibiotic against pneumonia (Huynh et al., 2024), pharyngitis (Pereira et al., 2018), sepsis, and many other types (Kaur et al., 2011). Although AMX has therapeutic efficacy, its presence in water makes bacteria resistant to antibiotics; thus, treating infections becomes more complicated (Sodhi et al., 2021). The presence of amoxicillin in aquatic environments poses significant ecological threats that extend beyond immediate toxicity concerns. Recent studies have demonstrated that even sub-therapeutic concentrations of AMX (as low as µg/L levels) can disrupt aquatic microbial communities, leading to the development of antibiotic-resistant bacteria and the horizontal transfer of resistance genes (Rodriguez-Mozaz et al., 2020; Carvalho and Santos, 2016). The persistence of AMX in water bodies has been linked to adverse effects on non-target organisms, including algae growth inhibition, disruption of fish reproductive systems, and alteration of ecosystem biodiversity (aus der Beek et al., 2016; Kümmerer, 2009). Furthermore, the World Health Organization has identified antimicrobial resistance as one of the top global public health threats, with environmental contamination being a critical pathway for resistance development (WHO, 2021). The ecological footprint of pharmaceutical contamination extends to drinking water sources, potentially affecting human health through chronic low-level exposure (Prasse et al., 2015). Therefore, the development of sustainable and cost-effective treatment technologies, such as the waste-derived adsorbent presented in this study, represents a crucial step toward mitigating these environmental challenges while simultaneously addressing waste management issues.

Removing AMX from water is considered a necessity as its water-soluble, weakly polyprotic nature, high chemical stability, hinders biodegradation, and potential hepatotoxic effects linked to flucloxacillin cell disruption (Pasamontes et al., 2004: Längin, et al., 2009: Kim et al., 2009). The existence of AMX in water could be related to its excretion in urine, with a high percentage (more than 70%) of the taken dose within the first two hours after its administration (Todd et al.,1990). Since AMX does not metabolize to fewer effective components, only a small portion will be converted to penicillanic acid in the liver (Delemos et al., 2016). AMX has been specifically targeted based on the Europium watch list for union-wide monitoring in the field of water policy. Four recently identified antibiotics, trimethoprim, sulfamethoxazole, ciprofloxacin, and AMX as pollutants that pose risks to the aquatic environment (Decision 2015). Several methods were utilized to remove AMX: photocatalytic systems, electro-oxidation, advanced oxidation processes, and ultrasonic systems (Qutob et al., 2022). Photocatalytic systems are stable and easy to use but consume high energy, while electrooxidation offers high efficiency but faces eco-toxicity and cost issues. Adsorption is effective and low-energy (Qutob et al., 2022, Moradi et al., 2020, Habibi et al., 2021, Brillas, 2022, Anjum, 2017]; therefore, it is considered a quite successful option to be used for removal of such compound. Many materials are used as adsorbents to remove AMX, including natural materials such as modified bentonite (Mohammed et al., 2024), activated carbon (Abbas and Trari, 2024), ionic liquids (Velho et al., 2024), nano-modified zinc oxide (Bousmaha et al., 2024), bio-composite containing magnetic chitosan (Mirizadeh et al., 2024), carbon nanomaterials such as carbon nanotubes (Hussaini et al., 2024), also adsorbents containing binary metals (Ashraf et al., 2024). To maintain the cost-effectiveness of the adsorption process, it is common to utilize waste-derived materials as adsorbents, irrespective of their origin. Industrial by-products such as cement kiln dust (CKD), zero-valent iron, sewage sludge from water treatment plants (Faisal et al., 2022a), and gypsum-derived plaster kiln dust (Hussein, Faisal, 2023) are frequently employed, addressing both waste management and adsorption efficiency challenges. CKD is considered a modifiable source of calcium that has been used in various studies, such as by converting it to hydroxyapatite (Faisal et al., 2021). This confirms the suitability of CKD for preparing new materials to act as effective sorbents. To achieve the minimal cost in the preparation of sorbent, water treatment sludge (WTS) was used as a source of aluminum, as this waste contains aluminum hydroxide that is produced from the added aluminum sulfate in the settling tanks (as a coagulant) (Huang, Shiu, 1996). Annually, huge amounts (millions of tons) of WTS are formed, usually disposed of as by-products in landfill (Nguyen et al., 2022). Previous studies demonstrate that the water treatment plants in the UK alone annually produce more than 180000 dry tons of WTS (Keeley, 2014). In Australian, the cost of safely disposing of sludge generated during the water treatment process is approximately \$130 per ton, resulting in an annual expenditure of \$6.2 million for disposal. The huge quantities of this waste require attention to utilize it in various applications, including adsorption and chemical modification. Recent studies are concentrated on management of reusing aluminum from WTS to remove pollutants from wastewater, which showed excellent results (Jangkorn et al., 2011). The WTS was utilized in phosphate adsorption studies, achieving superior results with sorption capacities of 30.83–34.53 mg/g (Xu et al., 2009). Among the promising materials as adsorbents are LDHs, which are a class of chemical compounds with a structure similar to brucite [$Mg(OH)_2$] in which the divalent ion is partially removed with a trivalent ion, producing a positive charge with the inner layer being mediated by a negatively charged ion and water molecules. The working formula for LDH: $[M_{1}{}^{2+}{}_{-X}M^{3+}{}_{X}(OH)_2]^{x}+[(A^{n-})_{x/n}.\,yH_2O]$; where M^{2+} is divalent metal cation (e.g., Mg^{2+}, Zn^{2+}, Ca^{2+}), $M^{3+}$is trivalent metal cation (e.g., Al^{3+}, Fe^{3+}, Cr^{3+}), and A^{n-} is exchangeable interlayer anion (e.g.,

CO_3^{2-}, NO_3^-, Cl^-, SO_4^{2-}). x: Fraction of trivalent metal cations, typically ranging from 0.2 to 0.33 (Shi et al., 2024).

LDH sorbents offer significant advantages, including the ability to tailor their constituent elements for specific applications, straightforward preparation methods, and operational versatility across a broad temperature range. The non-toxic and biocompatible nature makes them highly suitable for environmentally sensitive applications (Bai et al., 2024). The previous investigations demonstrate the possibility of extracting aluminum from WTS at a suitable pH, as long as the optimum pH is 2.5 (Altalhi et al., 2024; Panswad, Chamnan, 1992). A significant contribution of this study is the utilization of CKD waste as a calcium source, leveraging its established efficacy in pollutant removal. CKD-sand composite has demonstrated effectiveness in extracting heavy metals, such as copper and zinc, from acidic aqueous solutions, highlighting its potential for sustainable waste management and water treatment applications (Sulaymon et al., 2015). LDH-iron and magnesium composites have proven effective in removing estrogen (Abdul-Kareem et al., 2023). This work's specific objectives are to: (i) manufacture new reactive material called (Ca/Al) LDH-sodium alginate beads and determine its properties; (ii) investigate AMX adsorption onto the prepared beads; and (iii) assess the performance of this composite sorbent under various operating conditions. Popular models, batch studies, and characterization analyses can all be used to achieve these goals.

MATERIALS AND METHODS

AMX stock solution

State company of Drugs Industry and Medical Appliances in Samarra (Iraq) was supplied the AMX antibiotic used as target contaminant in this work. 1000 milligrams of AMX has polluted one liter of aqueous solution. Drops of 0.1 M HCl and NaOH are required to correct the acidity of this solution, also known as the stock solution, which was kept at room temperature. To get the necessary concentration of the target contaminant in batch tests, the stock solution must be diluted. An Ultraviolet–visible (UV)–visible spectrophotometer (Model Shimadzu 1100, Japan) set to 227 nm wavelength is used to test AMX concentrations.

Cement kiln dust (CKD)

The CKD was collected from the Kirkuk cement factory in Iraq. Ten kilograms were collected, divided, quartered, and crushed to a size (70 µm). The powder was chemically analyzed to check the percentages of major elements, as shown in Table 1.

Water treatment sludge (WTS)

Ten liters of water treatment sludge were collected from Al-Weihda water treatment plant (from sedimentation tanks) in Baghdad, Iraq. The sludge was exposed to air for 3 days in summer (45 °C) for drying. It was crushed to 70 µm. The powder was chemically analyzed to find the ratio of Aluminum as Al_2O_3 in the sludge, as shown in Table 1.

Extraction of Ca and Al ions

For the extraction of calcium ions, 40 ml HCl (25%) was added carefully to 10 g CKD powder under ambient temperature and stirred at 250 rpm. The CO_2 gas was released immediately, proving the chloride ion substitution from HCl. After the finishing of CKD addition, the mixture was left on a stirrer for 30 minutes. The color of the solution changed to yellow and then to yellowish orange. The mixture was filtered and washed, and the supernatant (Ca^{+2}) was collected for the next step. The same procedure was applied for the extraction of Al^{+3} from WTS using 20 g of WTS. The solutions of Al^{+3} and Ca^{+2} that had been prepared previously were mixed (as fresh solutions) under vigorous stirring for 15 minutes to give the main liquid for the essential ions. Thereafter, 2 drops of Tween 18 (polysorbate) were added under vigorous stirring, and foam was produced within 2 minutes. From a burette with a flow rate of 1

Table 1. The chemical analysis of CKD and WTS

Com. %	SiO_2	Fe_2O_3	Al_2O_3	CaO	MgO	LO I	SO_3	K_2O	Na_2O	TiO_2
CKD	11.82	1.57	2.83	44.43	2.80	21.95	10.55	0.95	1.00	0.25
WTS	37.98	4.11	20.30	5.40	0.45	30.02	1.21	0.22	0.31	nil

drop/second, 1 M solution of NaOH was added under vigorous stirring (700 rpm) to prevent any aggregations. Through this process, the pH was 1.2 and raised through the addition of NaOH until it was 8, and the mixture was thick. When the pH equaled 10, the solution was diluted (the pH effect was also studied for 7, 10, and 12). Then, the mixture was left stirring at room temperature for an additional 1 h to complete the reaction. The product was then collected by centrifuge at 4000 rpm for 5 minutes; thereafter, washed with hot water and centrifuged (the washing process was repeated until the pH equaled 7.5) and dried in an oven overnight at 50 °C. The same procedure was applied using different ratios of Ca: Al, to be 0.5:1 and 2:1.

Production of (Ca/Al)-LDH-sodium alginate beads

The 2 g of sodium alginate powder (Sigma Aldrich, MDL no.: MFCD00081310) was dissolved in 100 ml of deionized water and stirred for 24 h at room temperature; a dense solution formed in a gel form. Different amounts of LDH of Ca:Al=1 (0.1, 0.2, 0.4, 0.8, and 1 g, as 5, 10, 20, 40, and 50%, respectively) were added to the alginate gel under ultrasound disrupting process (750 Watt) (Sonics, USA) for 15 min in an ice bath to obtain a homogenous mixture. The mixture was dropped by using 10 ml syringe of diameter 4 mm in a $CaCl_2$ solution for polymerization and formation of beads, after 1 h curing in 1% solution of $CaCl_2$. The beads were collected using filter paper; then, rinsed twice with distilled water to remove excess $CaCl_2$. The (Ca/Al)-LDH-alginate beads were dried at 40 °C for 1 h. The removal efficiencies of AMX are using the prepared adsorbent, considered the distinctive indicator for assessing the effectiveness of the mixing process as a function of Ca:Al ratio, pH of the mixture, and LDH ratio in alginate.

BATCH OPERATION MODE (CA/AL)-LDH-ALGINATE BEADS

The following conditions: pH (2, 4, 7, 9, and 12), stirring speed (50–300 rpm), contact time (5, 10, 15, 20, 40, 60, 90, 120, and 180 min), AMX concentration (30, 50, 100, and 250 mg/L), and sorbent amount (1, 2.5, 5, and 7.5 g) were used to determine the optimums for removing AMX from polluted water. In a 250 ml conical flask, 50 ml of contaminated water was added with a specific amount of (Ca/Al)-LDH-alginate beads. The shaker was operated at a specific speed. After a certain time, the mixture was filtered through a 0.11 μm filter. The concentration of AMX was examined at the maximum wavelength of 227 nm. Using following equations, the amount of contaminant retained in the (Ca/Al)-LDH-alginate beads, $q_{e,}$ and the removal percent R%), were calculated:

$$q_e = (C_o - C_e)\frac{V}{m} \tag{1}$$

$$R\% = \frac{C_o - C_e}{C_o} \times 100 \tag{2}$$

where: C_o is the initial concentration of contaminant, C_e is the contaminant concentration at the equilibrium, V is the sample volume, and m is the adsorbent mass.

MODELING OF THE SORPTION OUTCOMES

Adsorption isotherms

The mathematical basis for adsorption is an isotherm models that express the distribution of contaminant concentrations between solid particles and the liquid phase at a state of equilibrium for a specific temperature. Two equilibrium relationships are applied as explained below (Hussein, Faisal 2023):

1. Freundlich isotherm model

$$q_e = K_f Ce^{1/n} \tag{3}$$

where: n is the sorption intensity, and K_f is an indicator of adsorption capacity.

2. Langmuir isotherm model

$$q_e = \frac{q_{max} bCe}{1 + bCe} \tag{4}$$

where: q_{max} is the highest capacity of sorption, and b is the affinity between contaminant and sorbent.

Kinetic relationships

To ascertain the contaminant's uptake rate, a kinetic analysis is necessary in order to establish residence duration in the sorption system, design an appropriate sorption method, and understand the governing sorption mechanisms. The present sorption measurements have been subjected to two kinetic expressions (Hussein, Faisal 2023):

3. Pseudo first order

$$q_t = q_e(1 - \mathrm{e})^{k_1 \mathrm{t}} \tag{5}$$

4. Pseudo-second order

$$q_t = \frac{1}{\left(\frac{1}{(k_2 q_e^2} + \frac{1}{q_e}\right)} \tag{6}$$

where: q_t is the adsorbed contaminant at time (mg/g), q_e is the adsorbed contaminant at equilibrium (mg/g), k_x is the rate constant for first (x=1, min^{-1}) or second order (x=2, $\mathrm{g.mg^{-1}.min^{-1}}$).

RESULTS AND DISCUSSION

Manufacturing of (Ca/Al)-LDH-alginate beads

Since it is possible to obtain LDH by mixing Ca:Al ions in an alkali medium, this ratio and the pH that yield the desired compound were studied. The LDH was encapsulated in alginate at different ratios to determine the optimum conditions for achieving the highest removal of AMX at 50 mg/L. The optimum ratio for the reaction between Ca and Al was verified as three weight ratios (0.5:1, 1:1, and 1:2). The preparation of LDH was carried out at a pH of 7. It was added at a rate of 20% to the alginate and using (50 ml) of a solution at 50 mg/L AMX with room temperature for 60 minutes; however, the outputs have plotted in Figure 1a. The results prove that the optimal ratio is 1:1, followed

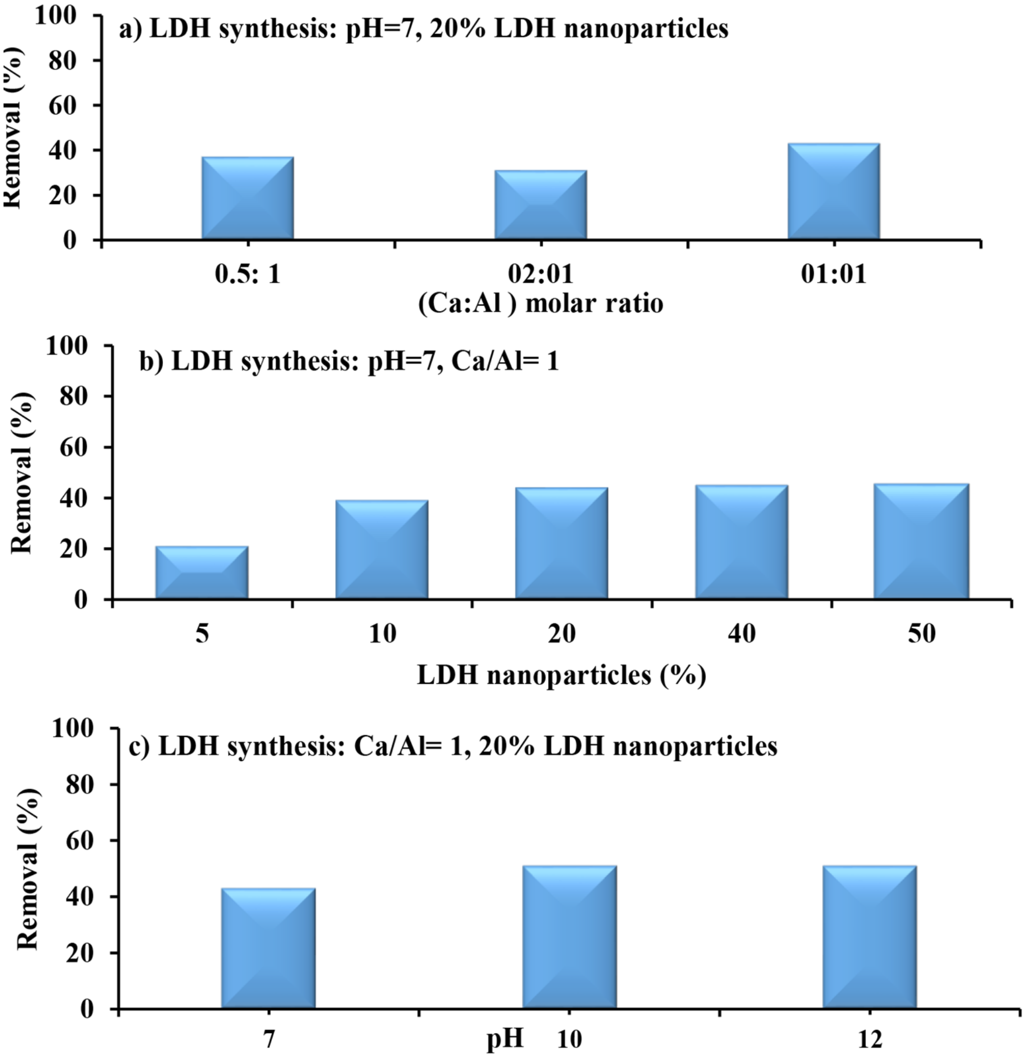

Figure 1. The effect of (a) Ca/Al ratio, (b) LDH nanoparticles percentage, and (c) pH on the AMX removal (sorption conditions; 50 ml of 50 mg/L AMX, dosage 0.5 g, 60 min, 25 °C, pH=7, speed 250 rpm)

by 0.5:1 and finally 2:1 due to the introduction of ions within the LDH structure formed, causing an obstacle to the adsorption of AMX. The reason is that a 1:1 ratio gave the ideal LDH structure without retaining additional ions between the active interlayers. The percentage of LDH in the alginate was investigated and the results have been plotted in Figure 1b. Ratios of 5–50 wt% were used; ratios beyond these values were not valid as the experiments did not give a homogeneous mixture by increasing the weight of LDH in the alginate. The removal of AMX is enhanced until it reaches 44% by increasing the ratio to 20% of LDH nanoparticles. This increase has an imperceptible positive effect on the adsorption efficiency. This indicates that increasing the ratio raises the flocculation of LDH in the polymer, reduces the percentage of active sites on the polymer surface, and thus reduces the removal of AMX antibiotic. The excess amount of LDH may not be attached to the alginate as it may be released with the beads' gelation or washing process (Ahmed, Faisal, 2023).

After determining the optimal ion ratio (Ca/Al=1) and the LDH ratio in alginate (20 wt%), the pH required to prepare LDH was studied in the range (7–12), considering that LDH does not form in acidic media. pH was chosen based on the basicity, where the mixture of reactants turns into a gel form. Approximately 52% of AMX was successfully removed (Figure 1c).

DESCRIPTION OF SYNTHESIZED MATERIALS

FT-IR measurements were examined to determine the functional groups for LDH-alginate beads (Figure 2(a)), LDH nanoparticles (Figure 2(b)), and LDH -alginate beads loaded with AMX (Figure 2c). Examination of calcium alginate beads shows that there is a band at 3425 cm^{-1} attributed to the stretching vibration for the hydroxyl groups in glucuronic and mannuronic acids, and since the number of these groups is large (8 in one alginate unit), the band broadening can be observed. The spectrum also shows two bands at 1470 and 1627 cm$^{-1,}$ supporting the presence of the symmetric and asymmetric stretching vibrations for the carboxylate ion, respectively. Finally, the band at 1130 cm^{-1} indicates the C-O-C groups; thus, the spectrum has confirmed the presence of alginate (Abdul-Kareem et al., 2023). In the FT-IR spectrum of LDH, the measurement illustrates the OH peak at 3411 cm^{-1} in the form of a broad band, indicating the conversion of calcium and aluminum ions to the corresponding hydroxide, enhancing the formation of the LDH. The bending vibration band at 1620 cm^{-1} is attributed to the water molecules that fill the inner layers of LDH through the interlayer hydrogen bonding. The stretching vibration bands of the hydroxide bonds appeared at 436 and 580 cm^{-1}, demonstrating the stretching vibrations of M-O, M-OH, and O-M-O, where M represents calcium and aluminum. For the spectrum of the alginate beads containing LDH, the spectrum showed a decrease in the intensity of the LDH bands, proving the formation of the required beads (Abdul-Kareem et al., 2023). Observation of alginate surfaces beyond AMX adsorption certified the formation of new peaks, like a peak at 991.232 cm$^{-1,}$ which is identical to the S-O vibrations, and the band at 1159.97 cm^{-1} resulted from C-N vibrations (–NH- CH$_2$-) in AMX (Abdul-Kareem et al., 2023)

The XRD test was conducted for CKD and LDH beads to identify the type of compound formed and its purity based on the location of the peaks and their number determines whether the

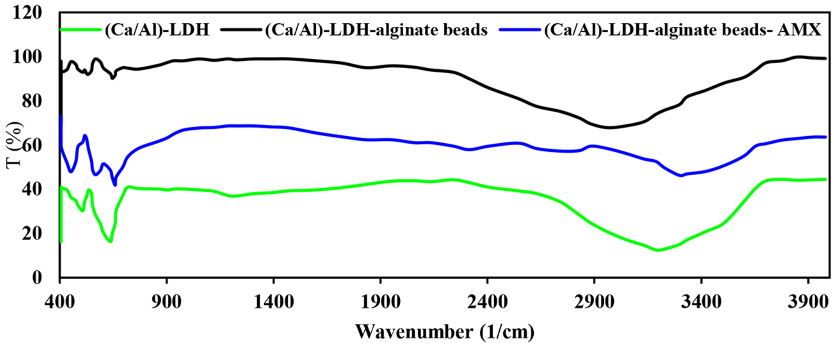

Figure 2. FT-IR analysis for (Ca/Al)-LDH-alginate beads, LDH nanoparticles, and (Ca/Al)-LDH-alginate beads loaded with AMX

compound is crystalline or amorphous. The test in Figure 3 showed that CKD consists of calcite $CaCO_3$, giving peaks at 23, 29.5, 36.5, 39.5, 43.0, and 48.5°, which agrees with JCPDS Card No. 05-0586 (Ma et al., 2013). The anhydrite (calcium sulfate) showed peaks as low-intensity peaks at 25.25, 31.5, 37, 36.5, 41.0, and 45.5° that agree with JCPDS Card No. 37-1496 (Nuraeni et al., 2019). The other components in the form of secondary compounds showed peaks at 27.1 and 34.0 degrees, attributed to quartz and portlandite (calcium hydroxide). This result is consistent with the chemical analysis in Table 1. In Figure 3, the LDH beads assay showed only six peaks at 11.4, 22.9, 31.32, 32.05, 55.2, and 56.8° attributed to the 002, 004, 110, 112, 030, and 032 crystal planes respectively that are identical to the compound prepared in the study conducted by Kim et al (Kim et al., 2012).

SEM and TEM were measured for the LDH beads to measure the morphology and size of the prepared LDH. SEM examination in Figure 4a showed the presence of nano-sheet-like particles with a thickness in the range of 50–56 nm in addition to the nano-rod structures with a diameter of 98–100 nm, indicating the formation of the LDH with its nano-sized and unique shapes that match those obtained in the literature (Ahmed, Faisal 2023). The proportion of sheets was higher than the proportion of rods compared to the previous study; this may enhance the role of the dispersing agent used. In TEM examination, the specific shapes appear more clearly as separate particles, as the diameter of the rod reached 20 nm, while the thickness of the sheet did not exceed 13 nm. When compared with the SEM result, the size is smaller, indicating that in SEM the particles appear as nano-aggregates, which were more accurately imaged in TEM in Figure 4b. Clear variations can be recognized in the sorbent morphology after interaction with AMX antibiotic, as shown in Figure 4c, due to the attachment of contaminant molecules.

To confirm the purity of the prepared compound, an EDX test of LDH was performed in Figure 5. The measurement showed the presence of oxygen, calcium, and aluminum in the composition, as well as a small percentage of sodium that can be attributed to a few residues from sodium hydroxide. The experimental ratios agree with the theoretical ratios (O; 47.37, Al; 19.97, and Ca: 29.67 wt.%), indicating the purity of the compound.

The information about the surface area of the prepared LDH was obtained by examining the N_2 adsorption-desorption isotherm (Figure 6). The surface area was 48.55 m^2/g, proving a large number of active sites available for adsorption. This value is higher than those recorded in previous studies, which demonstrates successful adsorption. The total pore volume reached 0.0512 cm^3/g, an appropriate value to accommodate AMX in the pores of the material, since AMX is a medium-sized molecule. The pore diameter is consistent with the total pore volume, reaching 22.35 nm. Finally, the BET constant value was 16.05, which indicates a strong correlation between LDH and AMX. This constant is higher than 10, for interactions occur effectively in adsorption.

The ideal conditions for the batch testing system

Studying the equilibrium between AMX and the active surface (adsorbent) is very crucial. The contact time factor is the most important to study before the rest of the factors, as it will provide

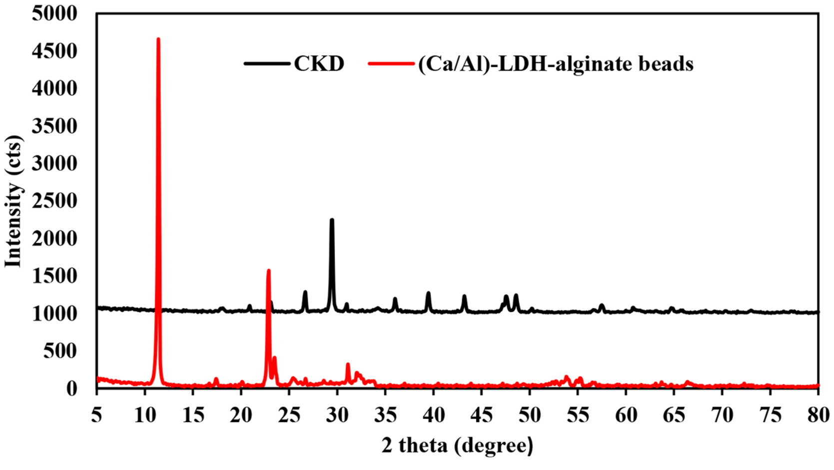

Figure 3. XRD analysis for CKD and (Ca/Al)-LDH

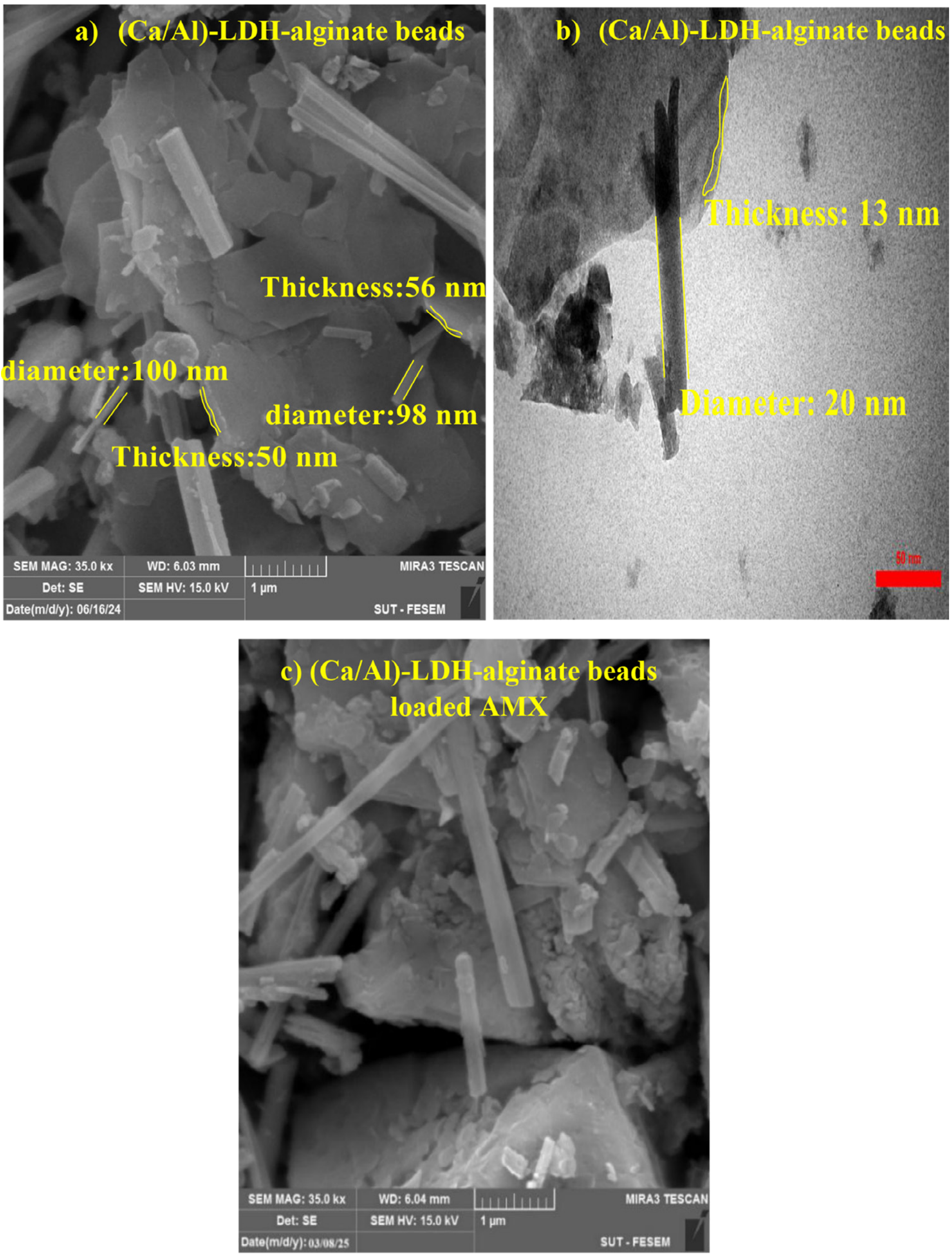

Figure 4. SEM image for virgin (Ca/Al)-LDH-alginate beads (a), TEM image for virgin (Ca/Al)-LDH-alginate beads (b), and SEM of (Ca/Al)-LDH-alginate beads loaded with amoxicillin antibiotic (c)

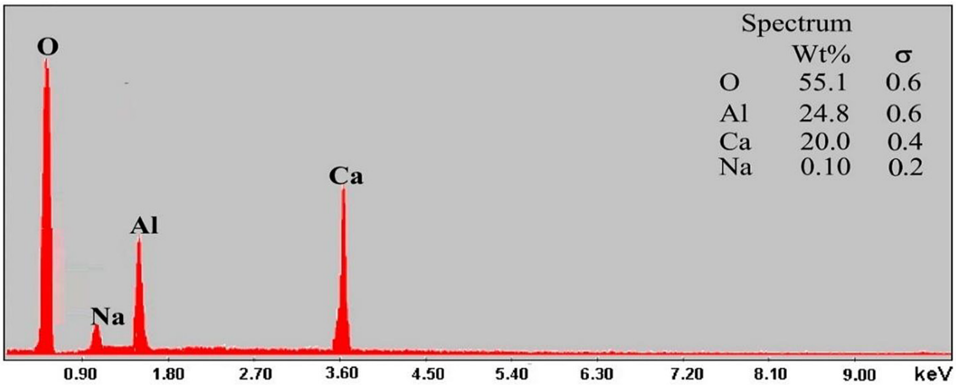

Figure 5. EDX analysis for (Ca/Al)-LDH

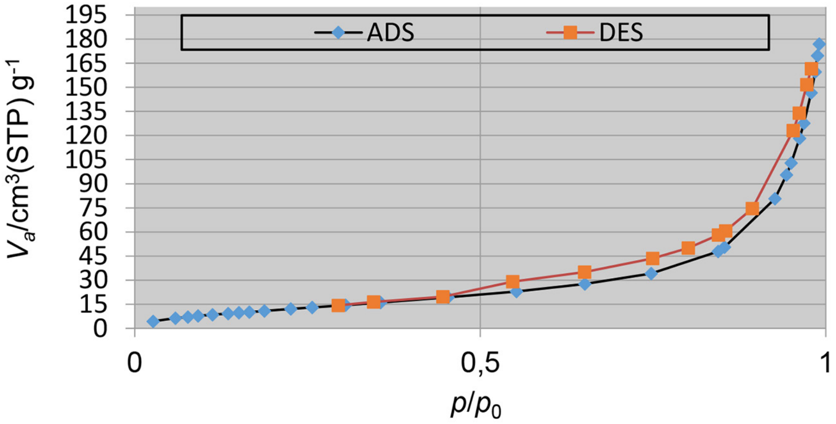

Figure 6. Measurement of surface area of (Ca/Al)-LDH by BET analysis

information related to the effectiveness of the adsorbent in removing the pollutant under study. The conditions used to study this factor were 50 mL of solution with AMX concentration 50 mg/L and an adsorbent amount of 0.5 g at pH 3. Figure 7a shows the effect of the contact time on the removal of AMX. Experiments have shown that with increasing contact time, the removal rate increases until it reaches the equilibrium time at 90 minutes with a removal value of 80%. These results state the rapid adsorption of AMX from the contaminated water (Faisal, Naji, 2019).

Since the removal of contaminant depends largely on the acidity function (pH), the effect of the acidity function on the removal of AMX was studied. AMX has three dissociation constants, one at 2.68, the second at 7.49, and the third at 9.63, attributed to the carboxylic, amino, and phenolic groups, respectively. The pH has a significant effect in activating the surface of the adsorbent and thus preparing it to interact with the antibiotic (Elhaci et al., 2021). Figure 7(b) shows the importance of the acidity function in the removal of AMX using 50 ml of solution contaminated with AMX at 50 mg/L and an adsorbent amount of 0.5 g for 90 minutes. At pH less than the dissociation constant of the carboxylic groups, the removal reached 64%, meaning that the surface of the adsorbent was charged with a positive charge with the conversion of the amine groups to NH^{+3}, causing repulsive forces that prevent high removal. At pH values of 3 and 4, AMX will be negatively charged by deprotonation of the carboxyl group, as well as a positive charge from the protonation of the amine, zwitterion of AMX is obtained. At this pH, the adsorbent is positively charged, and AMX will bind via its negative charge to the positively charged adsorbent (alginate-LDH). AMX carries an additional positive charge; the removal was not very high and reached a value of 86% at a pH value of 3. After that, the removal rate decreases due to the repulsion of the negative forces between AMX and the alginate-LDH until it reaches the lowest rate in basic media (Ahmed, Faisal 2023).

The effect of the initial concentration (10, 30, 50, 100, and 250 mg/L) of AMX on the removal rate was studied. AMX removal was carried out using 50 ml of AMX with an adsorbent amount of 500 mg at 90 minutes, pH equal to 3, and a shaking speed of 200 rpm. The results in Figure 7c using 50 mg/L give removal rates more than 81%, and then the removal rates decreased due to the increase in the amount of AMX spread in the solution (Ahmed, Faisal 2023).. The concentration of 50 mg/L was chosen as the optimal concentration because this rate will be considered an economical amount with a high removal rate compared to 10 and 30 mg/L. The effect of the shaking speed (50–250 rpm) on the removal of AMX was studied, as shown in Figure 7d. The optimum conditions determined from previous experiments were used in the study of this variable. The result showed that with increasing the shaking speed, the removal rate of AMX increases until it reaches 94% at 250 rpm. This is because rapid shaking makes the contaminant in ideal contact with the (Ca/Al)-LDH-alginate beads, with the possibility of causing penetration of AMX into the pores of the adsorbent (Ahmed, Faisal 2023: Amarasinghe, Williams, 2007). Finally, the amount of the (Ca/Al)-LDH-alginate beads was studied to determine its effect on the removal of

AMX, where weights of 100–750 mg of alginate containing LDH were used. When the adsorbent weight is 100 mg, the AMX removal was 78%, which gradually increases until it reaches 94% using 500 mg, after which there is only a slight raised (Ahmed, Faisal 2023: Amarasinghe, Williams, 2007). This results from the increase of active surfaces at which the removal and binding of AMX, which is represented in Figure 7e.

Modeling of sorption in a batch system

Sorption isotherms

To determine the migration of AMX (as a pollutant) in continuous mode of operation, Langmuir and the Freundlich isotherms were applied to formulate the sorption data and this is very important in the advection-dispersion equation. Figure 8 shows the concurrence between the

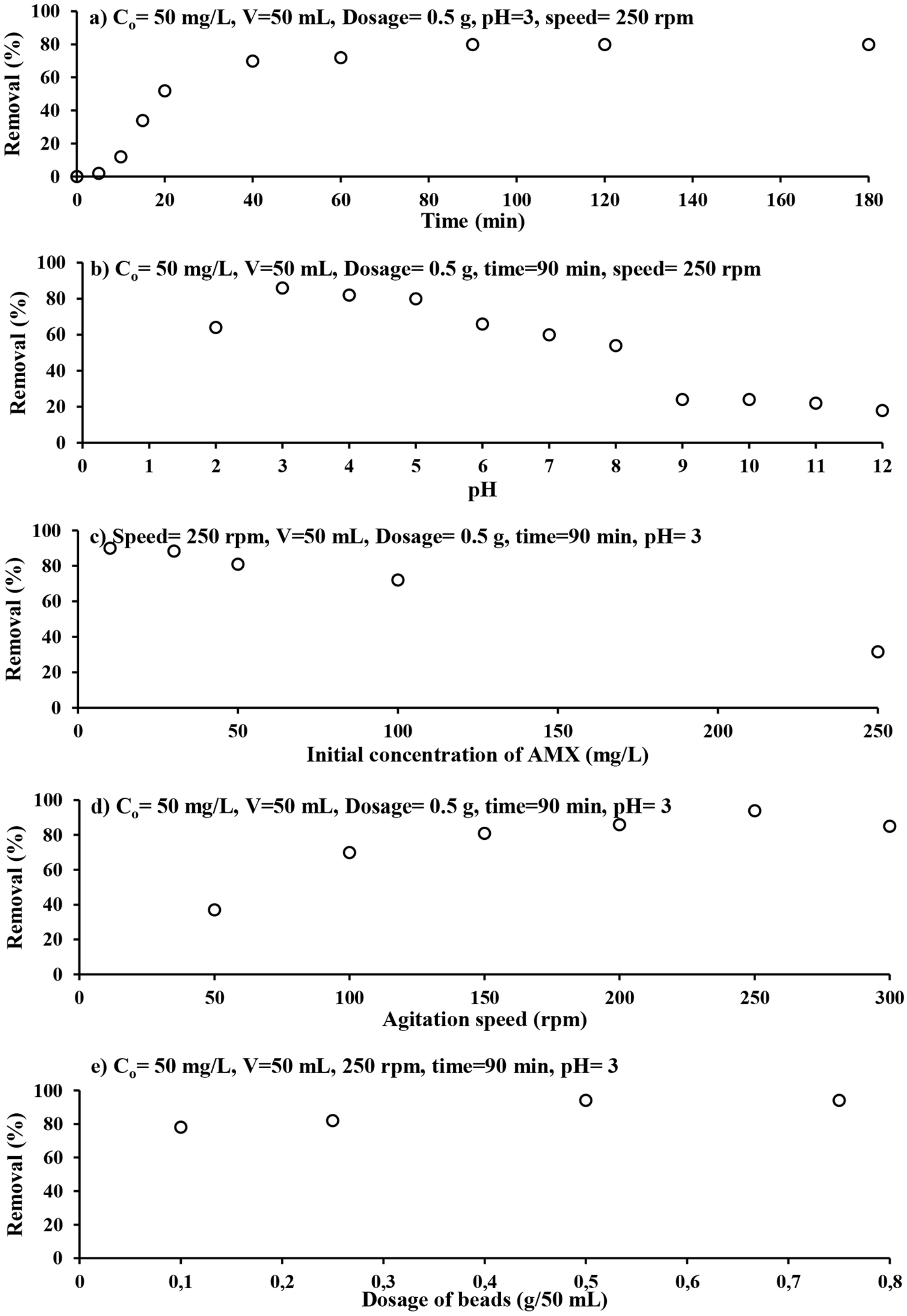

Figure 7. Effect of (a) contact time, (b) pH, (c) Co of AMX, (d) agitation speed, (e) dosage of (Ca/Al)-LDH-alginate beads

measurements and predictions calculated from Langmuir and Freundlich models depending on the Solver option in Microsoft Excel. The results of fitting (Table 2) showed that the R^2 values were 0.999 and 0.981 for Freundlich and Langmuir isotherms, respectively, indicating that both models describe the distribution of AMX onto (Ca/Al)-LDH-alginate beads meaning that it is within the surface and homogeneous diffusion. The calculations showed that the value of the Freundlich constant K_f reached 2.70 (mg/g)(L/mg)$^{1/n}$ with n of 2.991. Since this value is greater than 1 (Gheju, Miulescu, 2007), the adsorption process is favorable and refers to the adsorption capacity of a surface at low concentration of AMX. Through the Langmuir model, the q_{max} value was found to be 17.74 mg/g with b value less than 1, indicating a favorable interaction. The q_{max} value is considered one of the distinctive values compared to previous studies in Table 3.

Sorption kinetics

The kinetics provide information about the adsorption rate of AMX on the (Ca/Al)-LDH-alginate beads surfaces, thus providing information about the effect of contact time, which represents the rate of AMX transfer in the aqueous phase and its binding to (Ca/Al)-LDH-alginate beads. To determine this, the changes in q_e should be described as a function of time at the optimum conditions achieved in Table 2. Based on the Solver option, the adsorption kinetics results were obtained and illustrated in Table 2 and Figure 9. The results demonstrated that the adsorption rate is consistent with the pseudo-second-order, where the R^2 value reached 0.999 and SSE value of 0.1, indicating the occurrence of chemical adsorption of AMX with (Ca/Al)-LDH-alginate beads, while the R^2 value for the first order was 0.987. The second-order model suggests that the adsorption process is more dependent on the concentration of the adsorbate.

Recyclability

Ten cycles of regeneration for (Ca/Al)-LDH-alginate beads were tested. The adsorbent was activated by immersing it in hydrochloric acid at a concentration of 0.5 M (the use of HCl reflects the nature of chemisorption where low pH leads to protonation of the amine groups in AMX and changes the surface charge, facilitating desorbing). The results of recyclability are shown in Figure 10, where this adsorbent can be used for ten cycles without affecting its adsorption capacity by more than 8%, as it remained effective in removing approximately after ten cycles (86%). Experiments show that during the first five activations of the exhausted material, the removal rate was 94%, indicating that the activation has an effective effect, after which it decreases to the predetermined value at last cycle.

Mechanism of adsorption

The nature of the changes that occur on the surface of the (Ca/Al)-LDH-alginate beads due to interact with AMX antibiotic plays a major role in the adsorption mechanisms. In the prepared

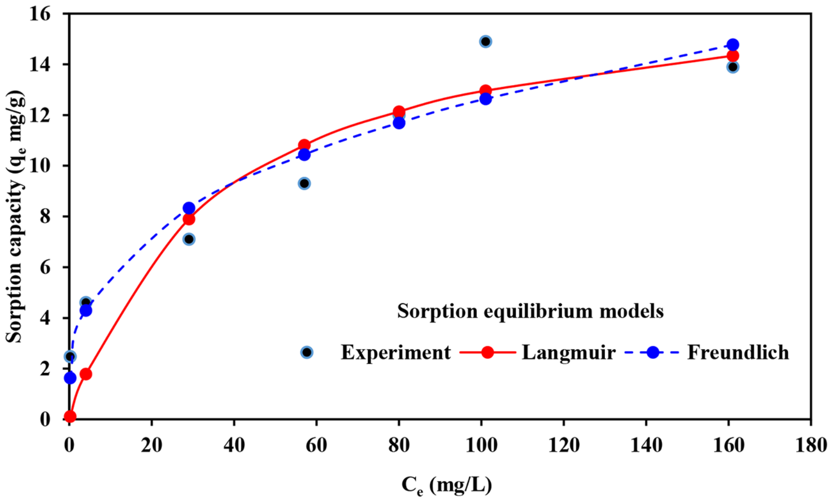

Figure 8. The isotherms for sorption of AMX onto (Ca/Al)-LDH-alginate beads in comparison with measurements

Table 2. Constant and statistical measures for Langmuir, Freundlich, first- and second-pseudo-order models

Model	Parameter	Value
Freundlich	K_f (mg/g)(L/mg)$^{1/n}$	2.70
	n	2.991
	R^2	0.999
Langmuir	q_{max} (mg/g)	17.47
	B	1.523
	R^2	0.981
Pseudo first order	q_e	4.743
	k_1 (min^{-1})	0.040
	R^2, SSE	0.987, 0.207
Pseudo-second order	q_e	5.706
	k_2 (mg/g min)	0.007
	R^2, SSE	0.999, 0.100

Table 3. Comparison of maximum adsorption capacity of AMX onto (Ca/Al)-LDH-alginate beads with other literature studies

Material	q_{max} (mg/g)	Reference
Activated carbon	4.4	(de Franco et al., 2017)
Vine wood carbon	2.69	(Pouretedal, Sadegh, 2014)
Chitosan beads	8.71	(Adriano et al., 2005)
Mg/Al LDH	32.42	(Elhaci et al., 2021)
(Ca/Al)-LDH-alginate beads	17.47	This study

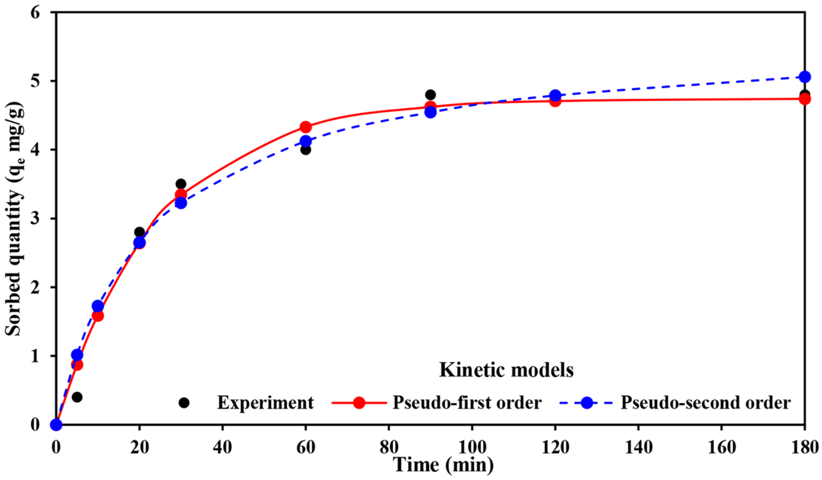

Figure 9. Formulation of AMX kinetic measurements onto LDH-alginate beads using kinetic models

adsorbent, aluminum and calcium ions dominate the adsorption properties, as it is characterized by the presence of positive surface charges in addition to internal anionic charges (Eniola et al., 2020). The study confirmed that the removal is most efficient at pH 3, then the formation of zwitterion will occur, carrying both positive charge by the amine and negative charge by the carboxyl. At this pH, the LDH will carry a positive charge on its surface. As a result, the process will include two mechanisms: the first is the chemical bonding of carboxyl groups with the positively charged surface, represented by aluminum and calcium ions. The second mechanism includes the ion exchange of negative charges with the anions in the LDH structure. Furthermore, the hydrogen bonding and

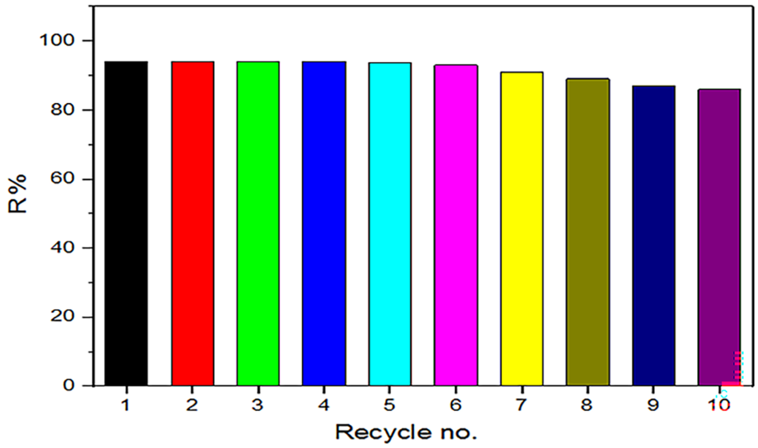

Figure 10. The effect of the regeneration cycles on the removal of AMX from contaminated water

adsorption on the surface are minor suggested mechanisms (Ahmed, Faisal, 2023; Eniola et al., 2020). Based on the fact that adsorption follows the pseudo-second-order, the first mechanism is the governing mechanism, as in Figure 11.

Economic analysis and cost comparison

While this study demonstrates the technical feasibility of using waste-derived (Ca/Al)-LDH-alginate beads for AMX removal, a preliminary economic assessment reveals promising cost advantages. The utilization of CKD and WTS as free waste materials significantly reduces raw material costs compared to conventional adsorbents. The primary cost components include sodium alginate (~15–20 \$/kg) and processing chemicals (HCl, NaOH ~2–5 \$/kg), while avoiding disposal costs for both waste streams. Compared to commercial activated carbon (2–5 \$/kg), advanced oxidation processes (0.5–2 \$/m³), and membrane technologies (0.3–1 \$/m³), the proposed method offers competitive economics, particularly when considering the 10-cycle regeneration capability

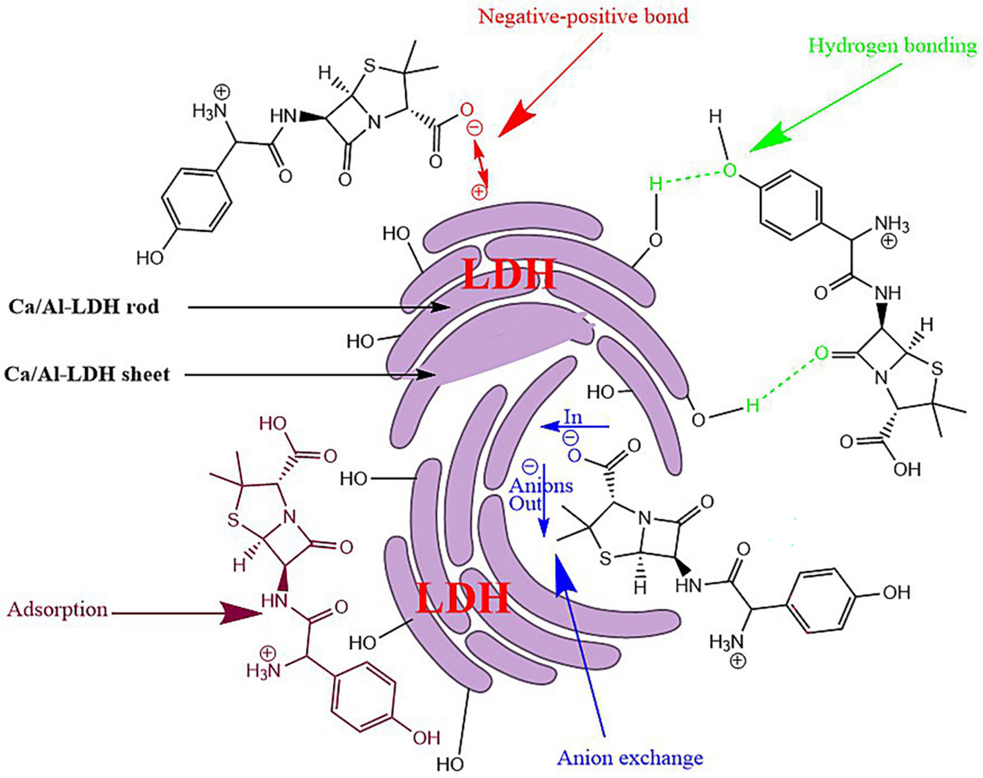

Figure 11. Proposed mechanisms for the removal of AMX using (Ca/Al)-LDH-alginate beads

and the dual environmental benefit of waste valorization. The estimated treatment cost is approximately 0.8–1.2 \$/m³, making it economically viable for developing countries where waste management and water treatment are critical challenges. However, comprehensive life-cycle cost analysis and pilot-scale economic validation are essential for definitive cost-benefit assessment and commercial implementation strategies.

CONCLUSIONS

This study proves the possibility of using CKD and WTS as sources of positive ions (Ca^{+2}, Al^{+3}) for the preparation of nano-sized LDH. The LDH nanoparticles can be immobilized by sodium alginate to prepare the (Ca/Al)-LDH-alginate beads. Additionally, the reaction conditions that achieve the highest adsorption results are pH 7, 20% LDH nanoparticles in alginate bead and Ca/Al=1. The (Ca/Al)-LDH beads have been characterized using FT-IR, XRD, SEM, EDX, TEM, and BET analyses. These tests showed the formation unique nano-shapes. The batch system demonstrates that the optimum conditions to achieve the highest removal of AMX (94%) were contact time (90 min), pH (3), shaking speed (250 rpm), and (Ca/Al)-LDH-alginate beads) (0.5 g) at AMX concentration of 50 mg/L. The adsorption isotherm study showed that the q_{max} value reached 17.47 mg/g, indicating the highest ability to remove AMX from polluted water. Adsorption kinetics demonstrated that the pseudo-second-order model provides an accurate description of the adsorption of AMX using (Ca/Al)-LDH-alginate beads; therefore, the chemical forces control the adsorption process. Future studies should focus on continuous column studies (permeable barrier), economic feasibility analysis, and the development of pilot-scale treatment systems to bridge the gap between laboratory findings and practical environmental applications.

REFERENCES

1. Abbas, M., Trari, M. (2024). Removal of amoxicillin from wastewater onto activated carbon: optimization of analytical parameters by response surface methodology. *Dose-Response*, *22*(3), https://doi.org/10.1177/15593258241271655
2. Abdul-Kareem, M. B., Rashid, H. M., Hassan, W. H., Al-Ansari, N., Lakhera, S. K., Hatshan, M. R., Faisal, A. A. (2023). Preparation of coated MgFe layered double hydroxide nanoparticles on cement kiln dust and intercalated with sodium dodecyl sulfate as an intermediate layer for the adsorption of estrogen from water. *Chemosphere*, *344*, 140338. https://doi.org/10.1016/j.chemosphere.2023.140338
3. Ahmed, Z. A., & Faisal, A. A. (2023). Precipitation of calcium-aluminum-cetyltrimethylammonium bromide nanoparticles on the sand to generate novel adsorbent for eliminating of amoxicillin from aquatic environment. *Alexandria Engineering Journal*, *66*, 489–503. https://doi.org/10.1016/j.aej.2022.11.019
4. Altalhi, A. A., Mohamed, E. A., Negm, N. A. (2024). Recent advances in layered double hydroxides (LDH)-based materials: Fabrications, modification strategies, characterization, promising environmental catalytic applications, and prospective aspects. *Energy Advances*. 3, 2136–2151. https://doi.org/10.1039/D4YA00272E
5. Amarasinghe, B.M.W.P.K., Williams, R.A., (2007) Tea waste as a low cost adsorbent for the removal of Cu and Pb from wastewater, *Chem. Eng. J. 132*, 299–309,
6. Anjum, A. (2017). Adsorption technology for removal of toxic pollutants. *Sustainable Heavy Metal Remediation: 2: Case studies*, 25–80. https://link.springer.com/chapter/10.1007/978-3-319-61146-4_2
7. Ashraf, I., Agarwal, A., Singh, N. B. (2024). Green synthesis of Fe–Cu nanoparticles on multiwalled carbon nanotubes for amoxicillin removal from aqueous solution using walnut husk extract. *Journal of Porous Materials*, 1–14. https://doi.org/10.1007/s10934-024-01640-6
8. aus der Beek, T., Weber, F. A., Bergmann, A., Hickmann, S., Ebert, I., Hein, A., Küster, A. (2016). Pharmaceuticals in the environment—Global occurrences and perspectives. *Environmental Toxicology and Chemistry, 35*(4), 823–835. https://doi.org/10.1002/etc.3339
9. Bai, J., Zhang, X., Wang, C., Li, X., Xu, Z., Jing, C., Jiang, Y. (2024). The adsorption-photocatalytic synergism of LDHs-based nanocomposites on the removal of pollutants in aqueous environment: A critical review. *Journal of Cleaner Production*, *436*, 140705. https://doi.org/10.1016/j.jclepro.2024.140705
10. Bousmaha, M., Kharroubi, B., Bezzerrouk, M. A., Pignon, B., Medjadi, R., Boutiche, M., Benaraba, R. (2024). Efficient removal of amoxicillin and methyl orange with antibacterial activity assessment via nanostructured ZnO coatings synthesized by ultrasonic spray pyrolysis method. *Ceramics International*, *50*(13), 23784–23793. https://doi.org/10.1016/j.ceramint.2024.04.104

11. Brillas, E. (2022). A critical review on ibuprofen removal from synthetic waters, natural waters, and real wastewaters by advanced oxidation processes. *Chemosphere*, *286*, 131849. https://doi.org/10.1016/j.chemosphere.2021.131849
12. Carvalho, I. T., Santos, L. (2016). Antibiotics in the aquatic environments: A review of the European scenario. *Environment International, 94*, 736–757. https://doi.org/10.1016/j.envint.2016.06.025
13. de Franco, M.A.E., de Carvalho, C.B., Bonetto, M.M., de Pelegrini Soares, R., Féris, L.A. (2017). Removal of amoxicillin from water by adsorption onto activated carbon in batch process and fixed bed column: Kinetics, isotherms, experimental design and breakthrough curves modelling. *J. Cleaner Production 161*, 947–956. https://doi.org/10.1016/j.jclepro.2017.05.197
14. Decision, E. U. (2015). 495/2015, Commission Implementing Decision (EU) 2015/495 of 20 March 2015 establishing a watch list of substances for Union-wide monitoring in the field of water policy pursuant to Directive 2008/105/EC of the European Parliament and of the Council. *Off. J. Eur. Union L*, *78*, 40-42. https://eur-lex.europa.eu/eli/dec_impl/2015/495/oj/eng
15. Delemos, A. S., Ghabril, M., Rockey, D. C., Gu, J., Barnhart, H. X., Fontana, R. J., Drug-Induced Liver Injury Network (DILIN). (2016). Amoxicillin–clavulanate-induced liver injury. *Digestive diseases and sciences*, *61*, 2406–2416. https://doi.org/10.1007/s10620-016-4121-6
16. Elhaci A., Labed F., Khenifi A., Bouberka Z., Kameche M., Benabbou K. (2021). MgAl-Layered double hydroxide for amoxicillin removal from aqueous media*, Int. J. Environ. Anal. Chem. 101*, 2876–2898, https://doi.org/10.1080/ 03067319.2020.1715374
17. Eniola, J. O., Kumar, R., Mohamed, O. A., Al-Rashdi, A. A., Barakat, M. A. (2020). Synthesis and characterization of CuFe2O4/NiMgAl-LDH composite for the efficient removal of oxytetracycline antibiotic. *Journal of Saudi Chemical Society*, *24*(1), 139–150. https://doi.org/10.1016/j.jscs.2019.11.001
18. Faisal A.A.H., Naji L.A. (2019). Simulation of ammonia nitrogen removal from simulated wastewater by sorption onto waste foundry sand using artificial neural network, *Assoc. Arab Univ, J Eng. Sci. 26*, 28–34, https://doi.org/ 10.33261/jaaru.2019.26.1.004
19. Faisal, A. A., Ahmed, D. N., Rezakazemi, M., Sivarajasekar, N., Sharma, G. (2021). Cost-effective composite prepared from sewage sludge waste and cement kiln dust as permeable reactive barrier to remediate simulated groundwater polluted with tetracycline. *Journal of Environmental Chemical Engineering*, *9*(3), 105194. https://doi.org/10.1016/j.jece.2021.105194
20. Faisal, A.A.H., Ahmed, D.N., Saleh, B., Afzal, A., Sharma, G., (2022a). Elimination of hazard cadmium ions from simulated groundwater using hydroxyapatite coated filter cake made of sewage sludge and cement kiln dust. *J. Polym. Environ. 30*, 1478–1490. https://doi. org/10.1007/s10924-021-02286-0
21. Habibi, B., Pashazadeh, A., Saghatforoush, L. A. (2021). Zn-mesoporous metal-organic framework incorporated with copper ions modified glassy carbon electrode: Electrocatalytic oxidation and determination of amoxicillin. *Microchemical Journal*, *164*, 106011. https://doi.org/10.1016/j.microc.2021.106011
22. Huang, C., Shiu, H. (1996). Interactions between alum and organics in coagulation. *Colloids and Surfaces A: Physicochemical and Engineering Aspects*, *113*(1–2), 155–163. https://doi.org/10.1016/0927-7757(96)03543-1
23. Hussaini, S. S., Hussain, M., Asim, M., Al-Balushi, A., Al-Saidi, B., Al-Ghafri, G., Seku, K. (2023). Facial synthesis of an efficient magnetic composite adsorbent using multiwalled carbon nanotubes and frankincense resin for the removal of amoxicillin pharmaceutical pollutants. *Journal of Molecular Liquids*, *390*, 123166. https://doi.org/10.1016/j.molliq.2023.123166
24. Hussein, T. S., Faisal, A. A. (2023). Nanoparticles of (calcium/aluminum/CTAB) layered double hydroxide immobilization onto iron slag for removing of cadmium ions from aqueous environment. *Arabian Journal of Chemistry*, *16*(9), 105031. https://doi.org/10.1016/j.arabjc.2023.105031
25. Huynh, D., Tung, N., Dam, Q., Tran, T., Hulten, K. G., Harrison, C. J., Le, J. (2024). Amoxicillin and penicillin G dosing in pediatric community-acquired pneumococcal pneumonia in the era of conjugate pneumococcal vaccines. *Pharmacotherapy: The Journal of Human Pharmacology and Drug Therapy*, *44*(8), 606–614. https://doi.org/10.1002/phar.2756
26. Jangkorn, S., Kuhakaew, S., Theantanoo, S., Klinla-Or, H., Sriwiriyarat, T. (2011). Evaluation of reusing alum sludge for the coagulation of industrial wastewater containing mixed anionic surfactants. *Journal of environmental sciences*, *23*(4), 587–594. https://doi.org/10.1016/S1001-0742(10)60451-2
27. Johnston, A. L., Lester, E., Williams, O., Gomes, R. L. (2021). Understanding Layered Double Hydroxide properties as sorbent materials for removing organic pollutants from environmental waters. *Journal of Environmental Chemical Engineering*, *9*(4), 105197 https://doi.org/10.1016/j.jece.2021.105197
28. Kaur, S. P., Rao, R., Nanda, S. A. N. J. U. (2011). Amoxicillin: a broad spectrum antibiotic. *Int J Pharm Pharm Sci*, *3*(3), 30–37. http://ijppsjournal.com/Vol3Issue3/2249.pdf

29. Keeley, J., Smith, A. D., Judd, S. J., Jarvis, P. (2014). Reuse of recovered coagulants in water treatment: an investigation on the effect coagulant purity has on treatment performance. *Separation and Purification Technology*, *131*, 69–78. https://doi.org/10.1016/j.seppur.2014.04.033
30. Kim, S. H., Saide, K., Farrell, J., Faulkner, L., Tailor, A., Ogese, M., Naisbitt, D. J. (2015). Characterization of amoxicillin-and clavulanic acid-specific T cells in patients with amoxicillin-clavulanate–induced liver injury. *Hepatology*, *62*(3), 887–899. https://onlinelibrary.wiley.com/doi/pdf/10.1002/hep.27912
31. Kim, T. H., Kim, H. J., Oh, J. M. (2012). Interlayer structure of bioactive molecule, 2-aminoethanesulfonate, intercalated into calcium-containing layered double hydroxides. *Journal of Nanomaterials*, *2012*(1), 987938. https://doi.org/10.1155/2012/987938
32. Kümmerer, K. (2009). Antibiotics in the aquatic environment–a review–part I. *Chemosphere, 75*(4), 417–434. https://doi.org/10.1016/j.chemosphere.2008.11.086
33. Längin, A., Alexy, R., König, A., Kümmerer, K. (2009). Deactivation and transformation products in biodegradability testing of ß-lactams amoxicillin and piperacillin. *Chemosphere*, *75*(3), 347–354. https://doi.org/10.1016/j.chemosphere.2008.12.032
34. Gheju, M., Miulescu, A. Sorption equilibrium of hexavalent chromium on granular activated carbon, (2007), *Chem. Bull. Politech. Univ. 52*(66) 41–46.
35. Ma, X., Yuan, S., Yang, L., Li, L., Zhang, X., Su, C., Wang, K. (2013). Fabrication and potential applications of $CaCO_3$–lentinan hybrid materials with hierarchical composite pore structure obtained by self-assembly of nanoparticles. *CrystEngComm, 15*(41), 8288–8299. https://doi.org/10.1039/C3CE41275J
36. Mirizadeh, S., Solisio, C., Converti, A., Casazza, A. A. (2024). Efficient removal of tetracycline, ciprofloxacin, and amoxicillin by novel magnetic chitosan/microalgae biocomposites. *Separation and Purification Technology, 329*, 125115. https://doi.org/10.1016/j.seppur.2023.125115
37. Mohammed, A. K., Saadoon, S. M., Abd Ali, Z. T., Rashid, I. M., Sbani, N. H. A. (2024). Removal of amoxicillin from contaminated water using modified bentonite as a reactive material. *Heliyon, 10*(3), e24916. https://doi.org/10.1016/j.heliyon.2024.e24916
38. Moradi, M., Elahinia, A., Vasseghian, Y., Dragoi, E. N., Omidi, F., Khaneghah, A. M. (2020). A review on pollutants removal by Sono-photo-Fenton processes. *Journal of Environmental Chemical Engineering, 8*(5), 104330. https://doi.org/10.1016/j.jece.2020.104330
39. Nguyen, M. D., Thomas, M., Surapaneni, A., Moon, E. M., Milne, N. A. (2022). Beneficial reuse of water treatment sludge in the context of circular economy. *Environmental Technology & Innovation, 28*, 102651. https://doi.org/10.1016/j.eti.2022.102651
40. Nuraeni, N., Kartikasari, D., Yani, S., Hiswara, E., Haryanto, F., Iskandar, F., Waris, A. (2019). Thermoluminescence characteristic of $CaSO_4$: Dy on β and γ radiation. *Journal of Physics: Conference Series, 1248*(1), 012081. https://doi.org/10.1088/1755-1315/1248/1/012081
41. Pasamontes, A., Callao, M. P. (2004). Determination of amoxicillin in pharmaceuticals using sequential injection analysis and multivariate curve resolution. *Analytica Chimica Acta, 515*(1), 159–165. https://doi.org/10.1016/j.aca.2004.01.005
42. Pereira, C. O., Ramos, D., Mação, P., Januário, G., Januário, L. (2018). Diagnosis and treatment of acute pharyngitis—is there any benefit on ten-day course of antibiotics? *Anales de Pediatría (English Edition), 88*(6), 335–339. https://doi.org/10.1016/j.anpede.2017.05.016
43. Pouretedal, H. R., Sadegh, N. (2014). Effective removal of Amoxicillin, Cephalexin, Tetracycline and Penicillin G from aqueous solutions using activated carbon nanoparticles prepared from vine wood. *Journal of Water Process Engineering, 1*, 64–73. https://doi.org/10.1016/j.jwpe.2014.03.006
44. Prasse, C., Ternes, T. (2010). Removal of organic and inorganic pollutants and pathogens from wastewater and drinking water using nanoparticles–a review. *Nanoparticles in the Water Cycle: Properties, Analysis and Environmental Relevance*, 55–79. https://doi.org/10.1007/978-3-642-10318-6_4
45. Qutob, M., Shakeel, F., Alam, P., Alshehri, S., Ghoneim, M. M., Rafatullah, M. (2022). A review of radical and non-radical degradation of amoxicillin by using different oxidation process systems. *Environmental Research, 214*, 113833. https://doi.org/10.1016/j.envres.2022.113833
46. Rodriguez-Mozaz, S., Chamorro, S., Marti, E., Huerta, B., Gros, M., Sànchez-Melsió, A.,... Barceló, D. (2015). Occurrence of antibiotics and antibiotic resistance genes in hospital and urban wastewaters and their impact on the receiving river. *Water Research, 69*, 234–242. https://doi.org/10.1016/j.watres.2014.11.021
47. Shi, Q., Cheng, M., Liu, Y., Wang, J., Zhang, G., Li, L., Liu, H. (2024). In-situ generated MOFs with supportive LDH substrates and their derivatives for photo-electrocatalytic energy production and electrochemical devices: Insights into synthesis, function, performance and mechanism. *Coordination Chemistry Reviews, 499*, 215500. https://doi.org/10.1016/j.ccr.2023.215500
48. Sodhi, K. K., Kumar, M., Singh, D. K. (2021). Insight into the amoxicillin resistance, ecotoxicity, and

remediation strategies. *Journal of Water Process Engineering, 39*, 101858. https://doi.org/10.1016/j.jwpe.2020.101858

49. Sulaymon, A. H., Faisal, A. A., Khaliefa, Q. M. (2015). Cement kiln dust (CKD)-filter sand permeable reactive barrier for the removal of Cu (II) and Zn (II) from simulated acidic groundwater. *Journal of Hazardous Materials, 297*, 160–172. https://doi.org/10.1016/j.jhazmat.2015.04.061
50. Todd, P. A., Benfield, P. (1990). Amoxicillin/clavulanic acid: an update of its antibacterial activity, pharmacokinetic properties and therapeutic use. *Drugs, 39*, 264–307. https://doi.org/10.2165/00003495-199039020-00008
51. Velho, P., Lopes, C., Macedo, E. A. (2024). Water Purification using choline-amino acid ionic liquids: removal of amoxicillin. *Industrial & Engineering Chemistry Research, 63*(8), 3654–3665. https://doi.org/10.1021/acs.iecr.3c04298
52. Xu, G. R., Yan, Z. C., Wang, Y. C., Wang, N. (2009). Recycle of Alum recovered from water treatment sludge in chemically enhanced primary treatment. *Journal of Hazardous Materials, 161*(2–3), 663–669. https://doi.org/10.1016/j.jhazmat.2008.04.008